Q. J. R. Meteorol. Soc. (2005), **131**, pp. 43–61 doi: 10.1256/qj.03.56B

Data assimilation of high-density observations. II: Impact on the forecast of the precipitation for the MAP/SOP IOP2b

By ROSSELLA FERRETTI[1,2*] and CLAUDIA FACCANI[1]

[1]*Department of Physics, University of L'Aquila, Italy*

[2]*CETEMPS, Center for the Forecast of Severe Weather by Remote Sensing and Numerical Modelling, Italy*

(Received 28 March 2003; revised 4 February 2004)

SUMMARY

The impact of the data assimilation of high-density (space and time) data on the precipitation forecast is evaluated by improving the initial conditions of a mesoscale model. The high-frequency data allow for improving the three-hourly initial and boundary conditions as well. The data assimilation is performed using initial objective analysis (Cressman and multiquadric schemes) and 3D-Var. The MM5 (version 3) mesoscale model from Penn State University/National Center for Atmospheric Research is used to evaluate the impact of the improved initial and boundary conditions on the model simulations. The comparison of model results with observations shows: (i) the forecast of the precipitation at high resolution produces better results than those without data assimilation only if three-hourly data are assimilated by multiquadric; (ii) the mean error of the model rainfall largely decreases only if 3D-Var is used, but no comparable improvement in the spatial distribution of the precipitation is found; (iii) the improvement for the rainfall is not as good as it is for the initial conditions for all experiments. Moreover, the observations ingested by objective analysis modify both the amount and the timing of the precipitation on the Po valley. On the other hand, 3D-Var modifies only the amount of the precipitation, but both techniques barely recover large-model failure.

KEYWORDS: Mesoscale modelling Model error Rainfall forecast

1. INTRODUCTION

Forecasting the precipitation in a complex orography area is still a challenging task. Both exact location and timing of the rainfall are difficult to forecast: a phase or position error is common in numerical models at a grid resolution of a few kilometres. Recently, Brewster (2003a) suggested a method to correct the phase error in the model simulation by using a field of shift vectors that minimize a squared error difference from high-resolution observations. Doppler radar data, i.e. radial component of the wind and the hydrometeor density, are used to that purpose. Brewster (2003b) found a positive impact in the location of a thunderstorm by applying the phase-correcting method at the time of the initial cell development. The results showed that the positive impact of the phase correction lasted for 3 h, but it is to be noted that a high-frequency data assimilation was performed. In this study a few model experiments are performed with the aim of exploring the impact of a high-density (space and time) dataset on the timing and position error of the rainfall for a test case. Faccani and Ferretti (2005, hereafter Part I) evaluated the impact of the data assimilation of a large amount of data recorded during the Mesoscale Alpine Programme (MAP) campaign on the initial conditions, for a case of Intense Observing Period (IOP) recorded between 19 and 21 September 1999 (IOP2b). In Part I, two data assimilation techniques are used: objective analysis (Benjamin and Seaman 1985; Nuss and Titley 1994) and 3D-Var (Barker *et al.* 2004). A large improvement (decrease of the mean error and standard deviation) of the initial condition is found if the multiquadric scheme and three-hourly data are used. In this paper, the same set of improved initial conditions, evaluated in Part I, is used to examine the impact of the data assimilation on the rainfall. The IOP2b is chosen, as already stated in Part I, because the moderate amount of rainfall

* Corresponding author: Department of Physics, University of L'Aquila, via Vetoio, 67100 L'Aquila, Italy.
e-mail: rossella.ferretti@aquila.infn.it

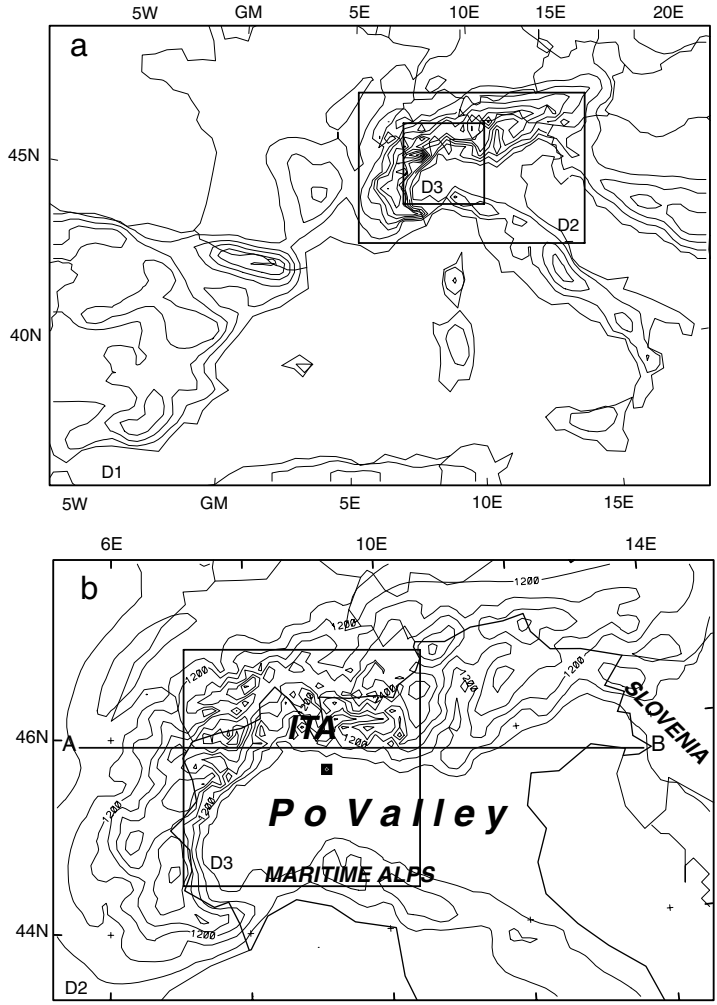

Figure 1. (a) Model domains: the grid size is $\Delta x = 27$ km for D1, $\Delta x = 9$ km for D2, and $\Delta x = 3$ km for D3; (b) Domains 2 and 3, and the line showing the location of vertical cross-section (from A to B) used in Fig. 10. The bold dot indicates Milano.

was mostly missed by all the operational models (http://map.ethz.ch and Ferretti *et al.* 2003b, hereafter FPO). The verification of the operational MM5 (version 2), from Penn State University/National Center for Atmospheric Research (PSU/NCAR), performed by FPO for most of the wet MAP cases showed a model tendency to underestimate the rainfall over flat terrain. Also Rotunno and Ferretti (2003, hereafter RF03) found a model tendency to underestimate the rainfall, using the same model as for FPO, even if the model was able to reproduce the local flow. Moreover, RF03 showed that the model recognized the differences between two IOPs (IOP2b and IOP8) that presented similar large-scale flow and large discrepancies in the local flow. In this paper, the relationship between the model shortcomings and the initial conditions will be examined. The MM5 model (version 3) is used to test the sensitivity of the model rainfall to the new initial conditions (Part I). The two model versions (2 and 3) are basically the same, but the major difference is in the interpolation technique used for the initialization procedure, therefore similar shortcomings are expected. A few high-resolution simulations are

performed, with the innermost model domain (D3 in Fig. 1) centred over the Italian Target Area (ITA in Fig. 1(b)). A comparison, such as the one performed for the initial conditions in Part I, is carried out to evaluate the impact of the data assimilation on the rainfall at high resolution. The rainfall differences between the observations and the model experiments, and a few statistical parameters (mean error and standard deviation) are used. An evaluation of the time evolution of the rainfall in the Po valley and on a cross-section taken along the same valley (Fig. 1(b)), is performed to better understand the MM5 shortcomings and the impact of the data assimilations techniques on the location error. The radar images are used for comparison.

A brief description of the meteorological characteristics of the IOP2b, the weather forecast experiments and the model configuration are presented in section 2. In section 3 the impact of the data assimilation on the model rainfall is evaluated. The time evolution of the model rainfall is discussed in section 4 and the conclusions are given in section 5.

2. THE CASE: METEOROLOGICAL ASPECTS AND NUMERICAL EXPERIMENTS

(*a*) *IOP2b meteorological characteristics*

A brief review of the meteorological characteristics of the IOP2b event (17–21 September 1999) is given. An exhaustive study of this case can be found in RF03 and Medina and Houze (2003). An upper-level trough, associated with a low pressure at the surface, entered ITA by 0600 UTC 20 September (Fig. 2(a)), advecting warm and moist air towards the south-western Alps (Fig. 2(b)). Moderate precipitation was recorded on the east side of the western Alps, moving eastwards during the day. This event shows large-scale meteorological characteristics (a deep upper-level trough with a tilted axis) similar to the ones of the Piedmont flood 1994 (Buzzi *et al.* 1998; Massacand *et al.* 1998; Rotunno and Ferretti 2001, hereafter RF01), but with less rainfall. During the MAP campaign, most of the operational models underestimated the total amount of rainfall, and particularly the MM5 model (version 2) completely missed the precipitation (RF03) near the city of Milano (bold dot point in Fig. 1(b)). The rainfall recorded during 20 September (Fig. 3(a)), in the western side of the Po valley, reached 200 mm, and moved quickly eastwards as shown in Fig. 3(b).

(*b*) *MM5 model set-up*

The MM5 model (version 3) from PSU/NCAR (Grell *et al.* 1994; Dudhia 1993) is used for this study. The MM5 is a non-hydrostatic model based on the primitive equations with a sigma terrain-following vertical coordinate. The model has multiple-nesting capabilities to enhance the resolution over the area of interest: the configuration is chosen to improve the forecast over ITA using three domains two-way nested (Fig. 1(a)). The mother domain has a grid size of 27 km and it is centred over the Mediterranean region. The grid resolution of domain 2 is 9 km, and the one of domain 3 is 3 km. The model configuration is basically the one used by Faccani *et al.* (2003): the Hong and Pan (1996) and Troen and Mahrt (1986) planetary boundary-layer parametrization is used; an explicit moisture scheme (Reisner *et al.* 1998) for all domains is associated to the Kain and Fritsch (1990) cumulus convection parametrization for D1 and D2 only. In addition, 29 unequally spaced vertical sigma levels, 1.00, 0.999, 0.995, 0.99, 0.98, 0.97, 0.96, 0.95, 0.94, 0.93, 0.92, 0.90, 0.85, 0.80, 0.75, 0.70, 0.65, 0.60, 0.55, 0.50, 0.45, 0.40, 0.35, 0.30, 0.25, 0.20, 0.15, 0.10, 0.05 and 0.00 are used.

The MM5 is initialized using the initial conditions generated in Part I. These allow for a few model experiments: CNTR, using the European Centre for Medium-Range Weather Forecasts (ECMWF) analyses; 6CRS, 6MQD, and 6h3D-Var using the

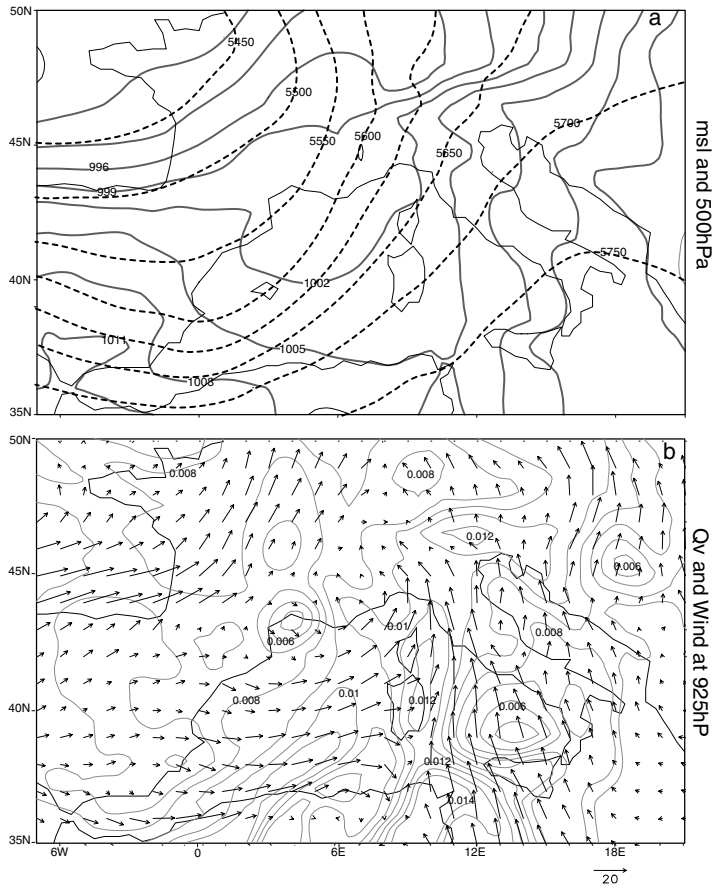

Figure 2. ECMWF analysis for 0600 UTC 20 September 1999: (a) mean-sea-level pressure (contour interval 3 hPa) and 500 hPa geopotentials (contour interval 50 m); (b) specific humidity (contour interval 2 g kg^{-1}) and wind vectors at 925 hPa (vector scale 20 m s^{-1} given by the arrow at the bottom of the panel).

ECMWF plus objective analysis or 3D-Var of six-hourly MAP data; 3CRS, 3MQD, and 3h3D-Var using the MM5-CNTR output, plus objective analysis or 3D-Var of three-hourly MAP observations. Further details regarding the initial conditions procedure can be found in Part I. All the experiments performed are in Table 1. Finally, the boundary conditions for I-CNTR and I-6 experiments are updated every 6 h, whereas for the I-3 experiments they are updated every 3 h.

The results from CNTR are used as reference. The comparison between CNTR and 6CRS, 6MQD and 6h3D-Var will enable the impact of a high-density network of observations to be evaluated. The comparison between the six-hourly and the three-hourly results will allow evaluation of the impact on the precipitation forecast of the high frequency updated boundary conditions. The comparison between Cressman, multiquadric, and 3D-Var for both six- and three-hourly data will enable the impact of the different techniques on the forecast to be evaluated. The results of all the experiments are compared with the observations. All the simulations start at 1200 UTC 19 September and they end after 48 h.

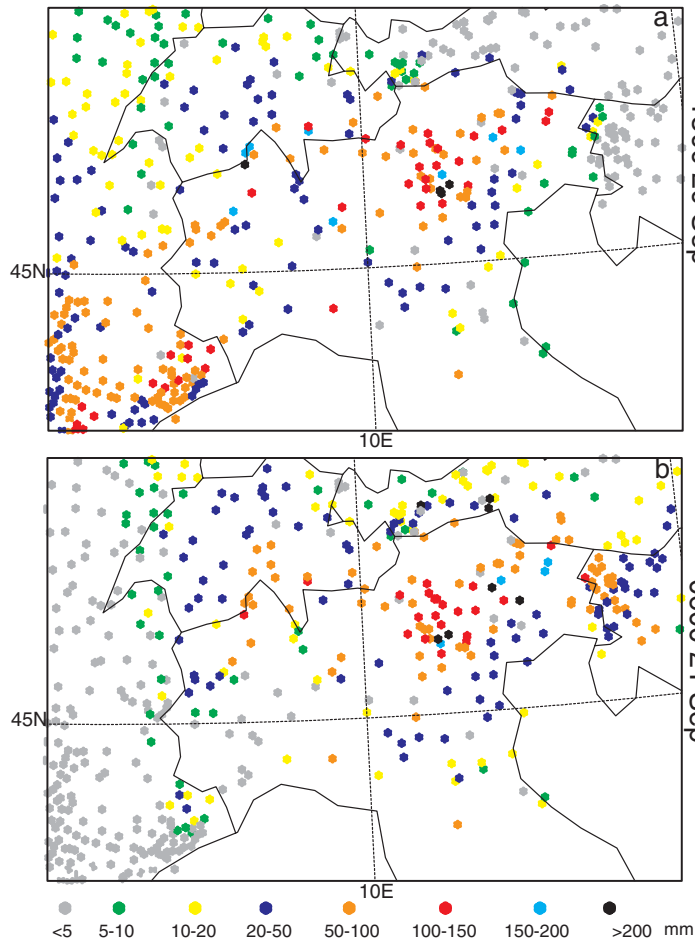

Figure 3. Observed 24 h accumulated precipitation during IOP2b ending at: (a) 1800 UTC 20 September, and (b) 0600 UTC 21 September.

TABLE 1. MM5 EXPERIMENTS PERFORMED USING THE INITIAL CONDITION GENERATED IN PART I: ECMWF DATA ANALYSES ARE USED FOR CNTR; DATA ASSIMILATION OF SIX-HOURLY DATA AND ECMWF ANALYSES ARE USED FOR 6CRS/6MQD AND 6H3D-VAR; DATA ASSIMILATION IS APPLIED USING MM5 OUTPUT AND THREE-HOURLY DATA FOR 3CRS/3MQD AND 3H3D-VAR

	Model experiment	Observations	Assimilation step
1	CNTR	no	–
2	6CRS-6MQD	yes	6 h
3	3CRS-3MQD	yes	3 h
4	6h3D-Var/3h3D-Var	yes	6 h/3 h

3. THE MODEL RESULTS

The impact of this special set of data on the high-resolution precipitation is evaluated: a comparison similar to the one performed for the initial conditions in Part I is carried out. The spatial distribution of the differences between the observed and the model rainfall at the station location and the corresponding scatter plots are examined.

The study will focus on the results in domain 2, because this domain is centred on the Po valley (Fig. 1(b)) where the rainfall phase error is found. Therefore, the results in domain 2 will allow for tracking the path of the rainfall during the simulation. However, this does not imply a low-resolution analysis because information from the higher-resolution domain (D3) is feedback to domain 2. To follow the evolution of the rainfall, two different periods are analysed: 24 h accumulated precipitation (Figs. 3(a) and (b)) ending at 1800 UTC 19 September (P1) and at 0600 UTC 20 September (P2). The heavy precipitation on the western side of the Po valley, recorded during P1 (Fig. 3(a)) moved quickly eastward during P2 (Fig. 3(b)). Heavy rainfall was recorded in the western Alps which exceeds 200 mm at the border with Switzerland (Fig. 3(a), the black dot). A moderate amount of rainfall was also recorded in the Po valley close to Milano (Fig. 3(a), red, orange and light blue dots west of 10°E). During P2, the maximum of the 24 h accumulated precipitation is recorded in the north-eastern Po valley (Fig. 3(b)): a large area of moderate precipitation (red dots) and a few stations recording more than 200 mm (black dots) are observed.

The hourly rain rate at the more significant time steps (0000, 0600, 0900, 1200, 1800 and 2100 UTC 20 September) is now examined, together with the rain rate estimated by the radar. The radar images are the product of a composition of a few radars operational during the MAP campaign (Alpine Composite, http://map.ethz.ch). The CNTR clearly reproduces the quick eastward evolution of the rainfall (Figs. 4(a1)–(f1); for ease of comparison the results of the model experiments, examined in section 6(c), are included) in crossing the western side of the Alps, and a good agreement is found between the hourly rain rate for CNTR (Figs. 4(a1) and (b1)), and the one by the radar (Figs. 4(a4) and (b4)). The 24 h accumulated precipitation reaches more than 200 mm (Fig. 5(a)) in good agreement with the observations (Fig. 3(a)). But a large underestimation of the 24 h accumulated precipitation is found along the Po valley close to Milano. The maximum for CNTR reaches 50 mm (Fig. 5(a), whereas the observation is up to 200 mm Fig. 3(a)) as already found by FPO, although the model version used for their work was the previous one (MM5 version 2). During P2, CNTR clearly shows a rapid eastward evolution of the rainfall (Figs. 4(c1) and (d1)) which was not observed (Figs. 4(c4) and (d4)); indeed, the observed rainfall continued over the central Po valley until 1800 UTC and then it moved quickly eastward (Figs. 4(e4) and (f4)). A consequence of the rapid evolution of the system produced by the model is a large underestimation of the 24 h accumulated precipitation: the maximum rainfall in this area reaches 100 mm (Fig. 5(b)). The MM5 shortcomings in correctly reproducing the precipitation along a valley was already found by FPO: they showed different values of the skill for the rainfall (see FPO, Figs. 7 and 8) on the mountain and flat areas. Therefore, the following examination will be performed keeping in mind this problem: the spatial distribution of the error (difference between the observations and the model rainfall) will be a help in understanding if the MM5 (version 3) still presents these shortcomings.

(*a*) *High-resolution rainfall for objective analysis*

The differences between the observation and CNTR clearly show a large underestimation of the precipitation over a wide area, in the north-eastern Po valley (east of 10°E and north of 45°N) and south-eastern France (Fig. 6(a)) during P1; whereas a small area of overestimation is found at approximately 12.5°E (Fig. 6(a), green and light blue dots). The objective analysis does not show a large impact: the underestimation of the precipitation is still present for both 6CRS (Fig. 6(b)) and 6MQD (Fig. 6(c)) in the north-eastern Po valley, and south-eastern France. But a large reduction of the error is found

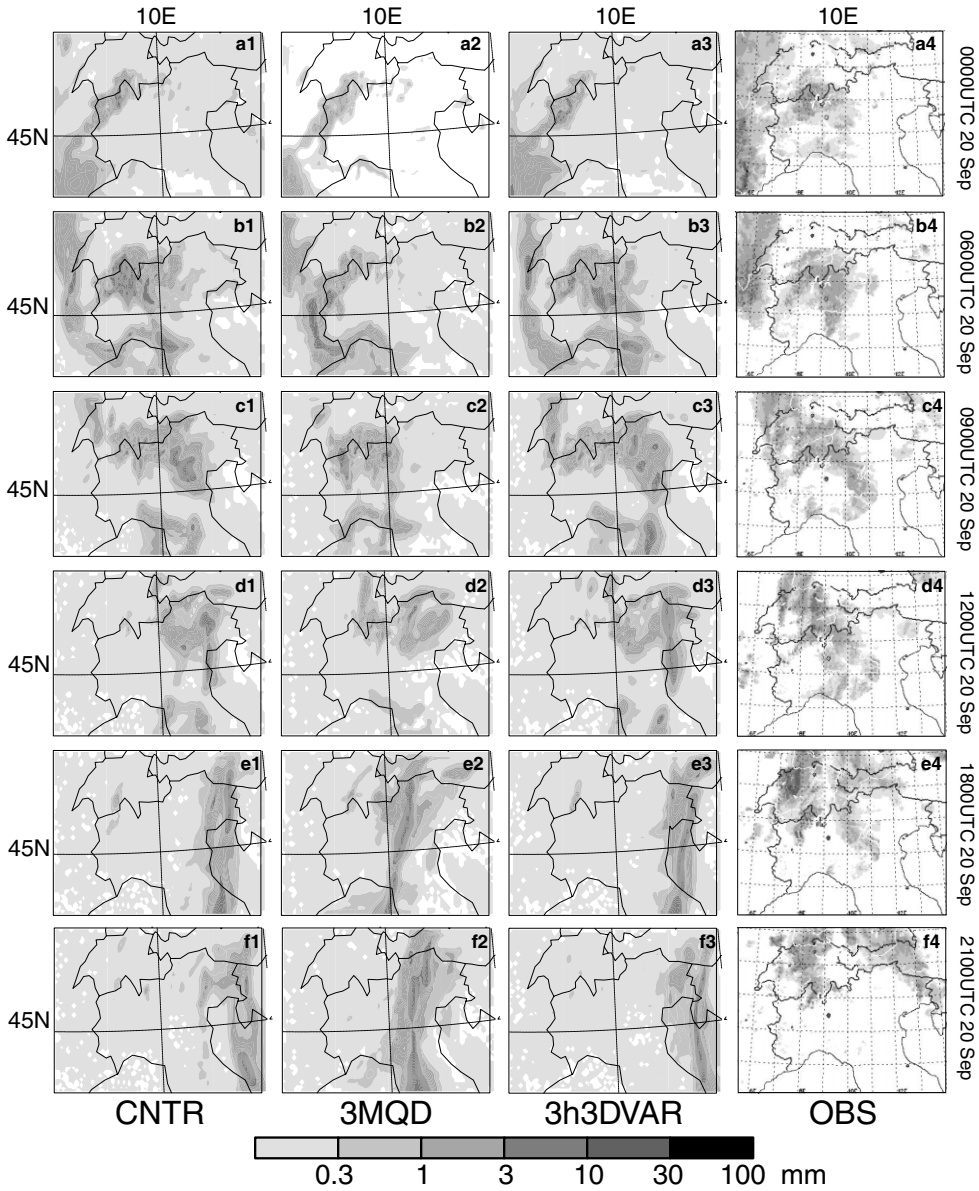

Figure 4. Hourly precipitation in domain 2 ending 20 September 1999: (a1)–(a4) 0000 UTC, (b1)–(b4) 0600 UTC, (c1)–(c4) 0900 UTC, (d1)–(d4) 1200 UTC, (e1–e4) 1800 UTC, and (f1)–(f4) 2100 UTC, for CNTR, 3MQD, 3h3D-Var and radar images.

for the small area of overestimation in the south-eastern Po valley (12.5°E, yellow dots) for 6MQD. Mostly, no remarkable differences are detected between 6CRS and 3CRS (not shown), and 6MQD and 3MDQ (not shown).

The scatter plots mainly confirm the previous results (Figs. 7(a1)–(a5)) for P1. Indeed, CNTR shows the tendency to underestimate the large amount of rainfall: the values are not aligned along the diagonal, but a general spreading is found (Fig. 7(a1)), especially for large values of the rainfall. The objective analysis produces a small reduction in the spread for the light rainfall for multiquadric only; on the other hand,

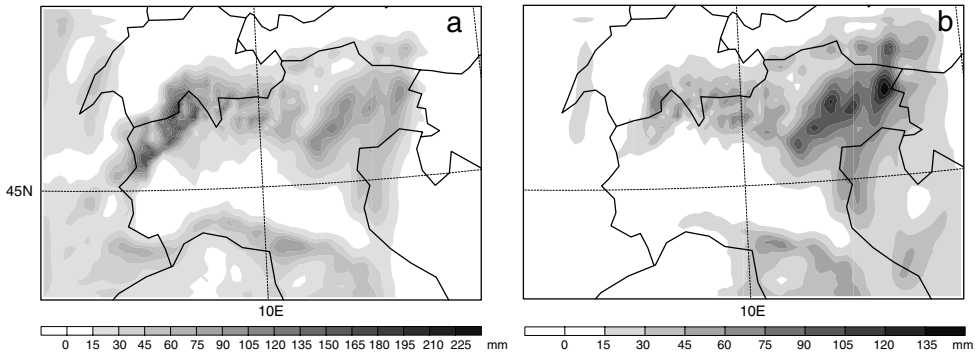

Figure 5. 24 h accumulated precipitation in domain 2 for CNTR, ending at: (a) 1800 UTC 20 September, and (b) 0600 UTC 21 September 1999.

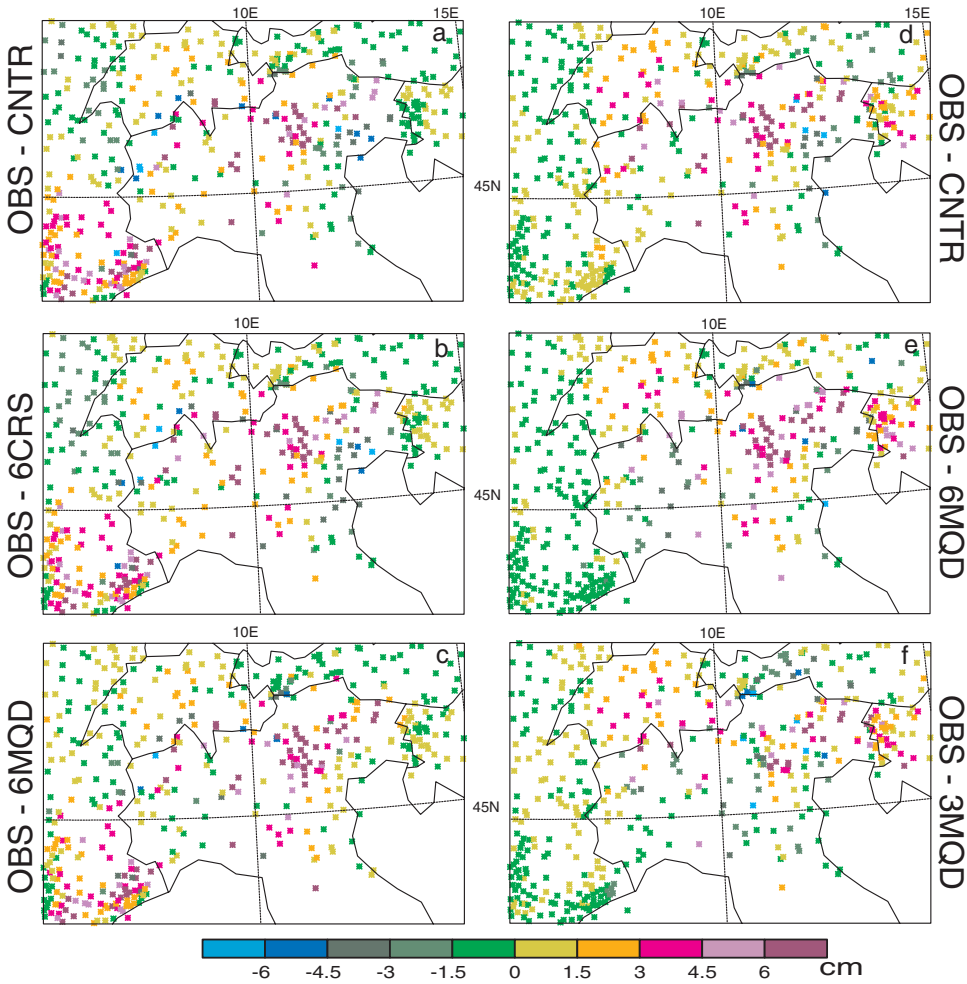

Figure 6. Differences (cm) between observation and model rainfall at rain-gauge location: time periods from 1800 UTC 18 September to 1800 UTC 19 September (P1) for (a) CNTR, (b) 6CRS, and (c) 6MQD; from 0600 UTC 19 September to 0600 UTC 20 September (P2) for (d) CNTR, (e) 6MQD, and (f) 3MQD.

the large rainfall is underestimated for both 6/3CRS and 6/3MQD (Figs. 7(a2), (a3), (a4) and (a5)). Mean error M and standard deviation STD mostly increase for all objective analysis experiments: 3MQD shows the highest value for $M = 16.11$, whereas the lowest one is obtained for CNTR, and only 6CRS shows the lowest value for STD $= 33.70$. The previous results show that, besides the large improvement of the initial conditions found in Part I, especially for 3MQD, a comparable improvement in the rainfall is not obtained for P1. A small reduction of the error in the area of Milano is found for 6MQD only, but the underestimation still persists.

The results show a different model response for all experiments during P2. The spatial distribution of the differences between observations and the model rainfall shows that the large error is still confined towards the eastern Po valley and western Slovenia (Fig. 1(b)) for CNTR (Fig. 6(d)). Both 6CRS and 3CRS (not shown) do not show any difference with respect to CNTR. The 6MQD shows (Fig. 6(e)) a small overestimation of the rainfall in the western Po valley (dark green, west of 10°E), and a large underestimation in the north-eastern Po valley and western Slovenia (red dots east of 10E and north of 45°N). Finally, 3MQD shows (Fig. 6(f)) a clear improvement of the rainfall, reducing the overestimation in south-eastern France (light green), and a reduction of the error is also found in the eastern Po valley and in western Slovenia (red and orange dots east of 10°E and north of 45°N).

The scatter plots show a spread distribution of the values, and an underestimation of the larger amount of rainfall for CNTR (Fig. 7(b1)) during P2. Both 6CRS and 6MQD do not show valuable improvement (Figs. 7(b2) and (b3)) of the error: still an underestimation of the large amount of precipitation is found. Also in this case, the statistical parameter confirms this finding: $M = 9.15$ for 6CRS and $M = 9.41$ for 6MQD as against $M = 9.57$ for CNTR. Also 3CRS does not show any improvement: the values are still spread for large amounts of rainfall (Figs. 7(b4)); in fact the corresponding mean error is the highest value ($M = 10.99$) with respect to all the other experiments, confirming these results. Finally, the best result is found for 3MQD: a narrower distribution (Fig. 7(b5)) than for all the other experiments is obtained, but the values are not completely aligned along the diagonal; $M = 4.94$ and STD $= 26.75$ confirm the improvement in the results.

(*b*) *High-resolution rainfall for 3D-Var*

During P1 the variational assimilation of six-hourly (6h3D-Var) data does not allow for improvement in the MM5 rainfall, on the contrary, an increase in the overestimation in the eastern Po valley is found (Fig. 8(a), light blue and blue dots close to the sea side 12.5°E and north of 45°N). A decrease in the error is found only along the border between Italy and Slovenia: CNTR produces an overestimation up to 4.5 cm (dark green), whereas 6h3D-Var dropped this value to 1.5 cm (light green). The assimilation of three-hourly data does not produce any improvement: 3h3D-Var produces a further overestimation of the rainfall in the eastern Po valley (Fig. 8b, dark green dots close to the sea side 12.5°E and north of 45°N), and a larger overestimation along the border between Italy and Slovenia (light blue dots).

During P2, a large reduction of the error is found in south-eastern France for both 6h3D-Var and 3h3D-Var (Figs. 8(c) and (d)), and also a reduction of the overestimation at the border between Italy and Slovenia is found for 3h3D-Var only. In contrast, 6h3D-Var produces an increase in the error (large underestimation) in the same area. In spite of the small improvement on the spatial distribution of the error, the scatter plots show remarkable impact of the data assimilation. A slightly closer distribution of the values along the diagonal for 6h3D-Var (Fig. 9(a)) than CNTR (Fig. 7(a1)) is found during P1.

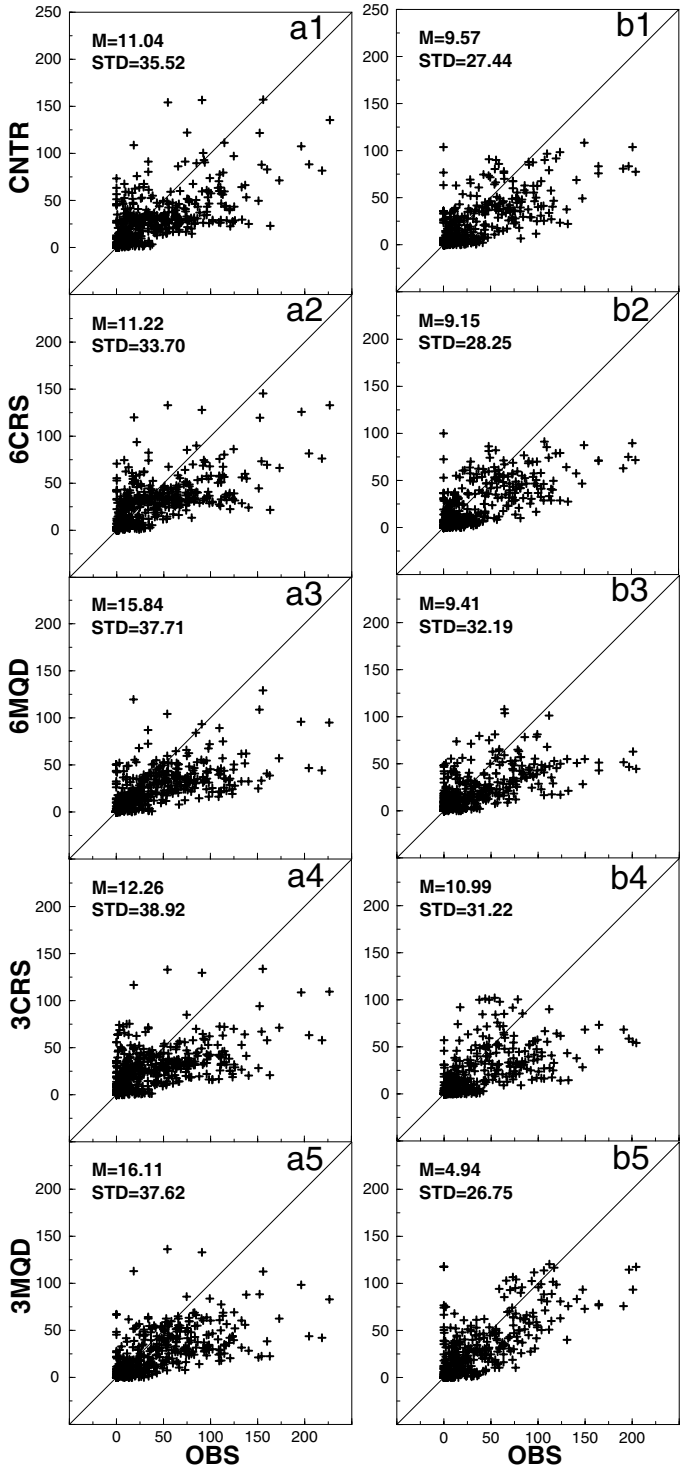

Figure 7. Scatter plots for observation and model rainfall (mm) for the two periods from 1800 UTC 18 September to 1800 UTC 19 September (P1, left column) and 0600 UTC 19 September to 0600 UTC 20 September (P2, right column) for: (a1)–(b1) CNTR, (a2)–(b2) 6CRS, (a3)–(b3) 6MQD, (a4)–(b4) 3CRS, and (a5)–(b5) 3MQD. Mean error M and standard deviation STD are also given.

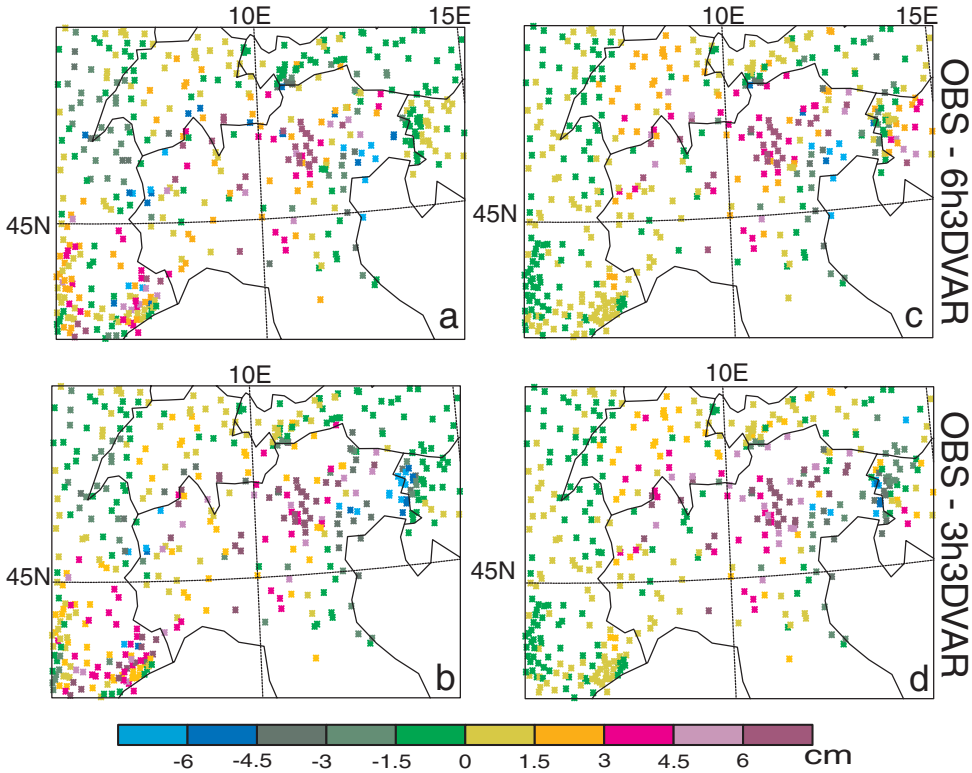

Figure 8. Differences (cm) between observation and model rainfall at rain-gauge location for time periods from 1800 UTC 18 September to 1800 UTC 19 September (P1, left column) and 0600 UTC 19 September to 0600 UTC 20 September (P2, right column) for: (a) and (c) 6h3D-Var, and (b) and (d) 3h3D-Var.

This result is strongly supported by the mean-error value ($M = 5.88$) that is almost half of the CNTR one ($M = 11.04$). This is the smallest value of the mean error with respect to all the other experiments during P1. The standard deviation also is smaller (STD = 33.65) than all the others, but the reduction is not as large as for M. The assimilation of three-hourly data (3h3D-Var) does not produce the same improvement as for the 6h3D-Var. The scatter plot (Fig. 9(b)) shows a larger underestimation for heavy rain than 6h3D-Var; this is confirmed by the mean error and the standard deviation ($M = 7.86$, STD = 38.14), that are both larger than the 6h3D-Var ones, but much smaller than both CNTR and all the objective analysis experiments.

During P2, again no remarkable differences are found between 6h3D-Var and 3h3D-Var (Figs. 9(c) and (d)): the scatter plots show similar distribution except for the model rainfall larger than 50 mm. For these values 3h3D-Var shows a larger spread than 6h3D-Var. Also the mean error and the standard deviation are similar: $M = 8.59$, STD = 28.74 for 6h3D-Var, and $M = 8.79$, STD = 32.10 for 3h3D-Var.

In summary, the previous results for both objective analysis and 3D-Var confirm the model shortcoming in correctly reproducing the precipitation along the Po valley; a clear underestimation of the precipitation close to Milano and in the north-eastern Po valley (approximately 12.5°E, north of 45°N) is obtained. Moreover, the precipitation in the central and north-eastern side of the Po valley is underestimated for both P1 and P2. Similarly, an underestimation of the rainfall in the same area is found by both FPO and RF03, but they also found that the model fairly estimated the precipitation in the

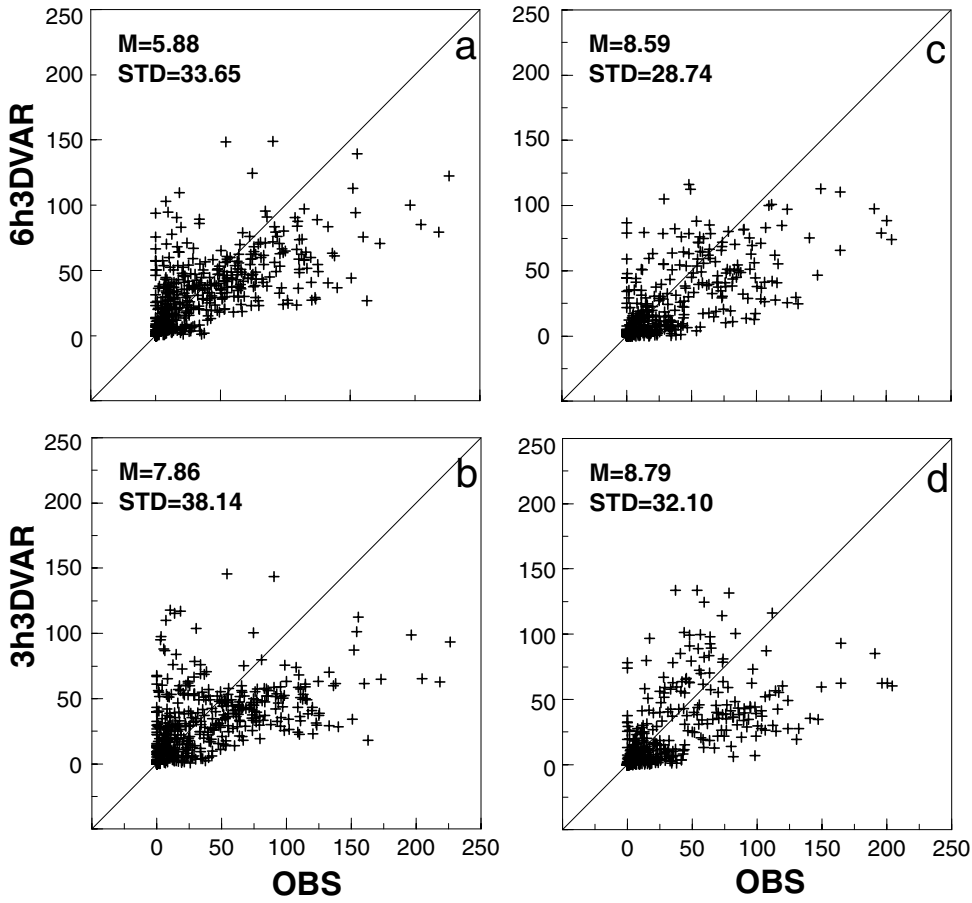

Figure 9. Scatter plots for observation and model rainfall (mm) for the time periods from 1800 UTC 18 September to 1800 UTC 19 September (P1, left column) and 0600 UTC 19 September to 0600 UTC 20 September (P2, right column) for: (a) and (c) 6h3D-Var, and (b) and (d) 3h3D-Var. Values for M and STD are given as in Fig. 7.

western Po valley (approximately at 8°E). Also in this work the precipitation in that area is fairly estimated by all the model experiments (with and without assimilation). During IOP2b the western Po valley was under the influence of an upslope wind (south-south-easterly wind), and a low-level easterly (RF03, Fig. 8(c)); the convergence of the southerly flow with the low-level easterly flow produced the uplift necessary to trigger the rainfall in this area. This suggests that the model needs a strong uplifting to trigger the precipitation which is not achieved on the flat terrain, i.e. along the Po valley. But also, a model tendency to move the rainfall along the Po valley too quickly may be responsible for the large underestimation of the precipitation. Moreover, an underestimation of either the strength of the westerly flow, or of the vertical velocity and the water-vapour content, may also contribute to the model failure in reproducing the rainfall. The large improvement in the estimation of the rainfall in the eastern Po valley (approximately 12.5°E, north of 45°N) close to the sea side, found for 3MQD, supports this hypothesis. Noteworthy is the small area of overestimated precipitation in the eastern Po valley (close to the sea side at 12.5°E and almost 45°N in Fig. 6(c), yellow and green dots), which corresponds to the area of a large overestimation found for specific humidity Qv and temperature T (Part I, Figs. 2(a) and (b) and Fig. 3).

The radiosoundings presented in Part I (their Figs. 10–13) clearly show a tendency for multiquadric to be closer to the observations, and almost an unstable or saturated atmosphere is observed for several locations. Therefore, a reduced stability produced by the overestimation of Qv and T, associated with the uplifting of the southerly flow (Fig. 2(b)) produced by the coastline, may be the cause of the overestimated rainfall in this area. It is to be pointed out that MM5 shows a tendency to overestimate the upward component of the vertical velocity as the flow crosses the coastline, as was recently shown by Ferretti *et al.* (2003a). As a consequence, the inland region (north-west of the one where overestimation of rainfall occurred) would experience a dryness because of a stable atmosphere produced by the downwind southerly flow from a precipitation area; this may explain the large underestimation of the rainfall in the north-eastern Po valley (at approximately 11.5°E and 46°N), reproduced by most of the experiments. The rain-shadowing effect, especially for Milano area, also may be blamed for model failure in reproducing the rainfall, as Colle *et al.* (1999) found in the western USA. Indeed, in this case Milano is located downwind to the southerly flow that produced precipitation in the Maritime Alps (Fig. 1(b)) during P1.

4. Evolution of the rainfall

The previous results clearly show a positive impact of objective analysis in correcting the model error for the rainfall if multiquadric is used. Similar results are found for 3D-Var if six-hourly boundary conditions are used. The model failure in reproducing the rainfall can also be related to the delay of the westerly flow in crossing the western Alps, due to too strong a barrier effect; on the other hand, a speeding up of the system moving eastwards along the Po valley produces an underestimation of the rainfall. To better understand this feature both the evolution of the spatial distribution of the hourly rainfall and its vertical structure are examined. This is done for both assimilation techniques; for objective analysis only the multiquadric scheme and for 3D-Var only the three-hourly experiment are presented. As found in Part I for the initial conditions and in this study for the rainfall, 3MQD is the one that gives the best results; whereas 3h3D-Var is the one that better reproduces the time evolution of the rainfall. The time evolution of the rainfall for CNTR has already been discussed (section 3(a)), therefore only the evolution of the data assimilation experiments is discussed. The hourly accumulated precipitation does show remarkable differences between CNTR and 3h3D-Var (Figs. 4(a1)–(c1) and (a3)–(c3)) during the first 9 h. The rain rate for 3h3D-Var closely reproduces the observed one (Figs. 4(a4)–(c4)); it is worth noting that 3D-Var is the only method able to produce rainfall close to Milano (Fig. 4(b3)). This is confirmed by the smallest mean error found during P1 for 3D-Var experiments. Unfortunately, during the following hours the system reaches the border between Italy and Slovenia by 1800 UTC 20 September, exiting the Po valley too early. On the other hand, objective analysis (3MQD) clearly shows a different time evolution of the hourly rainfall (Figs. 4(a2)–(f2)): at 1800 UTC 20 September the rainfall is still in the Po valley (closely east of 10°E). The rain rate estimated by the radar clearly shows (Figs. 4(a4)–(f4)) that the rainfall continues in the central Po valley for many hours (from 0600 to 1800 UTC 20 September).

The associated vertical structure on a cross-section (Fig. 1(b), from A to B), taken along the maximum rainfall in the Po valley, for the rain water at the same time steps of the hourly rain rate (Fig. 4), will help to understand the model behaviour. The CNTR (Figs. 10(a1)–(f1)) shows the rainfall, in the western side of the Po valley, slowly moving eastwards (approximately 100 km/6 h, Figs. 10(a1) and (b1)); it doubles the velocity (approximately 150 km/3 h, Figs. 10(b1) and (c1)) as it enters the valley, and

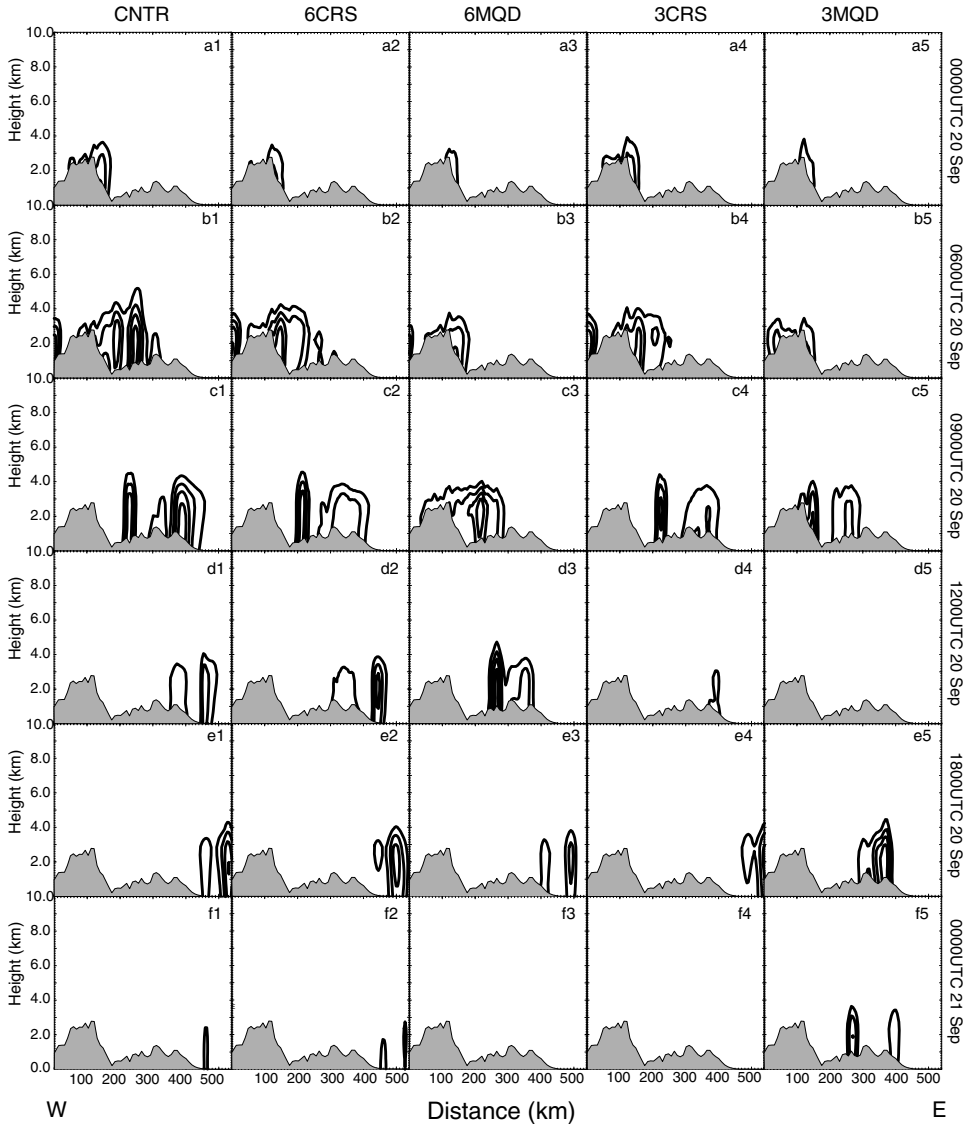

Figure 10. Cross-sections (line AB indicated in Fig. 1(b)) of rainwater (contour interval 0.25 g kg^{-1}) at: (a1)–(a5) 0000 UTC 20 September, (b1)–(b5) 0600 UTC 20 September, (c1)–(c5) 0900 UTC 20 September, (d1)–(d5) 1200 UTC 20 September, (e1)–(e5) 1800 UTC 20 September, and (f1)–(f5) 0000 UTC 21 September; for CNTR (first column), 6CRS (second column), 6MQD (third column) 3CRS (fourth column), and 3MQD (fifth column).

it largely reduces the rainfall and the speed in the next 9 h (Figs. 10(d1) and (e1)). As already shown, this evolution of the weather system in space and time produces a large underestimation of the rainfall in the central and north-eastern Po valley. The cross-sections for the objective analysis experiments show a different evolution for the rainfall depending on the time frequency of assimilation and the scheme used. The 6CRS rainfall (Figs. 10(a2) and (b2)), in the western side of the Po valley, is moving slightly more slowly (approximately 70 km/6 h) than CNTR: at 0600 UTC 20 September the maximum of the rainfall is delayed with respect to CNTR (Fig. 10(b1)). During the

passage along the Po valley (Figs. 10(b2) and (c2)), the velocity is largely increased (approximately 150 km/3 h) for 6CRS, producing no improvement in the rainfall as the differences of the accumulated precipitation between observations and 6CRS already showed for P1 (Fig. 6(b)). At 1200 UTC 20 September the rainfall produced by 6CRS (Fig. 10(d2)) is similar to CNTR. No remarkable differences are found for the last time steps (Figs. 10(e1), (e2), (f1) and (f2)). A large reduction of the velocity in the western Po valley (approximately 20 km/6 h) is found for 6MQD (Figs. 10(a3) and (b3)). This is associated with a reduction of the rainfall, as the increase of the error for the accumulated precipitation in this area suggests (Fig. 6(c), light green dots). The system moves slowly (approximately 60 km/3 h) eastwards (Figs. 10(b3) and (c3)) still underestimating the precipitation for 6MQD. In the following three hours (Figs. 10(c3) and (d3)) the system speeds up (approximately 100 km/3 h), but it is still delayed with respect to both 6CRS and CNTR at the same time (0900 UTC). At 1200 UTC 20 September the precipitation in the central Po valley is larger than both 6CRS and CNTR (Fig. 10(d3)); but this does not produce any improvement in the rainfall because of the short time of residence of the system in this area, as the large error for 6MQD would suggest (Fig. 6(c), magenta and purple points). In the following hours (Figs. 10(e3) and (f3)) the system rapidly moves eastwards, reaching the same location as for CNTR and 6CRS, but producing less precipitation than both of them. The assimilation of three-hourly data for Cressman (3CRS) does not produce remarkable changes for the system evolution in crossing the western Alps (approximately 60 km/6 h, Figs. 10(a4) and (b4)) with respect to 6CRS: their rainfall distributions are similar. In the next time step (0900 UTC) a reduction of the rainfall and a speeding up of the system (approximately 180 km/3 h, Figs. 10(b4) and (c4)), moving eastwards along the Po valley, still produces a large underestimation of the precipitation. The system exhausts earlier (Figs. 10(d4)–(f4)) than all the previous cases. The examination of the cross-section for 3MQD helps in understanding the poor results produced in the western side of the Po valley and the fair results obtained in the eastern side. The system produces little rainfall on the western side (Fig. 10(a5)) and it does not move eastwards in the first 6 h (Figs. 10(a5) and (b5)). In the following hours it slowly moves (approximately 80 h/3 h) eastwards, producing poor precipitation (Fig. 10(c5)). At 1200 UTC 20 September no rainfall is produced (Fig. 10(d5)), but it occurs in the following hours when the system reaches the eastern side of the Po valley (Figs. 10(e5)–(f5)), strongly reducing the error as the scatter plots and the error distribution show during P2. The cross-sections for both 6h3D-Var and 3h3D-Var (not shown) do not show remarkable differences and they are both similar to CNTR (Figs. 10(a1)–(f1)). The only difference found is slightly less rainfall at 0600 UTC 20 September. The 3D-Var is not able to correct the speeding up produced by the model; the time evolution of the meteorological system is the same as for CNTR. This is surprising because either the radiosoundings at the initial (Part I, Figs. 10–13) and following time steps (not shown), and the hourly rain rate show differences with respect to I-CNTR.

The radar images help in better evaluating the impact of objective analysis and 3D-Var on the evolution of the system. The radar clearly shows that the system slowly moved eastwards during the first 9 h (Figs. 4(a4)–(c4)): from 00000 to 0600 UTC 20 September it was stationary over the western Po valley (Figs. 4(a4) and (b4)); from 0600 to 0900 UTC of the same day it slowly moved (Figs. 4(b4) and (c4)) from the western to the central Po valley (approximately 50 km/3 h). The precipitation continued until 1800 UTC over this area (Figs. 4(d4) and (e4)), i.e. the system was almost stationary. In the following hours the system rapidly moved eastwards (approximately 400 km/12 h) reaching the east of the north-eastern Po valley by 2100 UTC 20 September. A moderate

amount of rainfall was recorded at 2100 UTC (Fig. 4(f4)) over the easternmost side of the Alps. The model tends to reproduce this feature as all the experiments show (Figs. 10 and 4). The comparison between the radar and both the model cross-sections and the hourly rainfall shows that CNTR moves the system eastwards too fast: as a consequence an underestimation of the precipitation is obtained. The objective analysis experiments only slow down the system moving eastwards, but neither 6CRS nor 3CRS succeeded in reproducing the correct speed. The only one able to correctly slow down the system is 3MQD. It shows a very slow-moving system in the western Po valley, which speeds up after 1800 UTC, and still produces precipitation at 2100 UTC at the border with Slovenia in agreement with the radar.

In summary, the previous results partially confirm what had already been found by Faccani *et al.* (2003) about the small impact of the data assimilation by objective analysis on the precipitation, in spite of the one obtained on the initial conditions. The data assimilation of high-density observations, in space and time, may correct the precipitation forecast only if three-hourly boundary conditions and the multiquadric scheme are used. This effect is mostly produced by a reduction of the initial error of the wind field and by filtering out the noise produced by the procedure applied using objective analysis. On the other hand, no correction on the speed moving eastwards and on the vertical structure of the rain is found if 3D-Var is applied. Instead, a large correction on the rain rate during the first phase (P1) of the event is obtained. This would suggest a positive impact of 3D-Var on the short-term forecast, produced by a local initial unbalancing of the flow and a vertical structure similar to the observed one. In Part I, the zonal and meridional components of the wind, U and V, show a large error suggesting a wrong balancing of the flow, which did not occur in the objective analysis experiments.

5. Conclusions

The results presented in this paper enable the impact of a large amount of observations on the precipitation forecast and on the model error to be evaluated using two data assimilation techniques: objective analysis and variational assimilation. The initial conditions, produced by applying both techniques (Part I), show a large reduction of the error on the surface data only if objective analysis is used. The model simulations performed using those initial conditions show a poor improvement in the rainfall for most of the experiments, except for 3D-Var. A large correction of the initial conditions by multiquadric was already found by Faccani *et al.* (2003) on the same area, but the rainfall did not show a comparable improvement. The results obtained in this study are in agreement with the previous work, suggesting that the assimilation of a large amount of data does not ensure an improvement of the rainfall. In spite of the general poor impact of objective analysis on the rainfall obtained by Faccani *et al.* (2003), in this study a remarkable improvement of the rainfall (24 h accumulated) during P2 is found for 3MQD. It is also to be pointed out that the statistical parameters (M and STD) show that CNTR has the lowest mean error and standard deviation for the 24 h accumulated precipitation with respect to the objective analysis experiments. In spite of the poor impact of 3D-Var on the initial conditions at the surface, the statistics of the rainfall (24 h accumulated) show that only 3D-Var is able to produce the smallest mean error and standard deviation, except for 3MQD for P2. Moreover, the hourly precipitation is well in phase with the observation during the first period of the event (P1). It confirms what had already been found by Barker *et al.* (2004), that 3D-Var does not produce

accurate initial conditions, but enables the model errors at the following time steps to be recovered.

Generally, all the model experiments show a tendency to underestimate the rainfall (24 h accumulated) in flat areas as already found by FPO. Moreover, the examination of both the hourly precipitation and the differences between the observations and the model rainfall enables the model shortcomings in correctly reproducing the speed of the system crossing the Po valley to be highlighted. They are related to the flow and the orography: the barrier effect by the western Alps, helps to retard the system moving eastwards in crossing the mountain ridge, recovering the effect of the underestimation of the easterly flow. The easterly flow itself acts to retard the system moving along the Po valley; therefore, a strong barrier effect may recover the impact of a light easterly wind. If the easterly flow is rightly estimated, it would enhance the underestimation of the rainfall (in the eastern side of the Po valley) because the convergence produced by the low-level easterly and southerly flows (in the west Po valley) would generate the right uplifting for triggering the precipitation in the western Po valley only (west of Milano in Fig. 1(b)). Indeed, a smaller error is found in this area than in the eastern side of the Po valley (east of 10°E), especially for 3D-Var experiments. As the system moves away from the western Alps and crosses the Po valley (east of 10°E), the model (CNTR) speeds up the system too much, producing an underestimation of the precipitation, due also to the short time of residence of the system in the area. As RF01 showed for this area, the precipitation is given, in first approximation, by the product of residence time and rainfall (see RF01, p. 1740); in this case the model tends to reduce the residence time too much. The effect of objective analysis by using multiquadric (3MQD) is to better control the speed of the system crossing the Po valley. It also has a larger impact on the region where the forcing produced by the convergence of both flows is small, as in central and eastern Po valley. Consequently, an increase of the rainfall is obtained, slowing down the velocity of the system, i.e. increasing the residence time. The rainfall is largely corrected by 3MQD in the south-eastern Po valley (close to the sea side at 12.5°E and almost 45°N in Fig. 6(c), yellow and green dots). The remarkable reduction of the error for the V component of the wind (reduction of the red dots along the Adriatic coast in the Balkan region in Fig. 5(d), Part I) allows the southerly flow to penetrate further inland from the Adriatic sea, reducing the precipitation along the coast, and increasing the inland one. Therefore, the assimilation of three-hourly data using multiquadric is the only one able to reproduce a rainfall (24 h accumulated) in good agreement with the observations. On the other hand, the effect of 3D-Var (6h3D-Var) is to correct the intensity of the instantaneous precipitation in the west side of the Po valley. As the system moves east no correction on the residence time of the precipitation and on the V component of the wind along the Adriatic sea is found. Indeed, 3D-Var does not allow for increasing the residence time, but the rainfall (24 h accumulated) is improved: M and STD values are lower than any other experiments, during P1.

These results strongly suggest that the two techniques, objective analysis and 3D-Var, produce different impacts on the physics, correcting the results in different ways. In fact the correction of the vertical structure of the rain is obtained only if multiquadric is used. This is in agreement with the correction produced by both techniques on the vertical structure of the atmosphere: at the initial time 3D-Var is closer to the observation than MQD, but the opposite is true at the following time steps. Two different phenomena may cause this effect: (i) the flow balance (geostrophic and cyclostrophic) performed by 3D-Var may filter out the correction introduced by the observations on the local flow; (ii) the ratio between horizontal and vertical density of the data, as Liu and Rabier (2003) suggested, is critical for having an impact on the vertical structure of the atmosphere.

Moreover, the 3D-Var shortcoming pointed out in Part I may contribute to reduce its positive impact on the model rainfall.

Acknowledgements

NCAR is acknowledged for the MM5 and special thanks to Dr Dale Barker and MMM Division for the 3D-Var code and their support. Graziano Giuliani is acknowledged for the program to extract the MM5 variables at the station locations. Prof. G. Visconti is gratefully acknowledged for supporting and encouraging this research. The two unknown reviewer are deeply acknowledged.

References

Barker, D. M., Bourgeois, A. J., Gou, Y.-R. and Huang, W. 2004 A three-dimensional variational data assimilation system for MM5: Implentation and initial results. *Mon. Weather Rev.*, **132,** 897–914

Benjamin, S. G. and Seaman, N. L. 1985 A simple scheme for objective analysis in curved flow. *Mon. Weather Rev.*, **113,** 1184–1198

Brewster, K. A. 2003a Phase-correcting data assimilation and application to storm-scale numerical weather prediction. Part I: Model description and simulation testing. *Mon. Weather Rev.*, **131,** 480–492

2003b Phase-correcting data assimilation and application to storm-scale numerical weather prediction. Part II: Application to a severe storm outbreak. *Mon. Weather Rev.*, **131,** 493–507

Buzzi, A., Tartaglione, N. and Malguzzi, P. 1998 Numerical simulations of the 1994 Piedmont flood: Role of orography and moist processes. *Mon. Weather Rev.*, **126,** 2369–2383

Colle, B., Westrick, K. J. and Mass, C. F. 1999 Evaluation of MM5 and Eta-10 precipitation forecasts over Pacific northwest during the cool season. *Weather and Forecasting*, **14,** 137–154

Dudhia, J. 1993 A non hydrostatic version of the Penn State-NCAR mesoscale model: Validation tests and simulation of an Atlantic cyclone and cold front. *Mon. Weather Rev.*, **121,** 1493–1513

Faccani, C. and Ferretti, R. 2005 Data assimilition of high-density observations: I. Impact on the initial conditions for the MAP/SOP IOP2b. *Q. J. R. Meteorol. Soc.*, **131,** 21–41

Faccani, C., Ferretti, R. and Visconti, G. 2003 High resolution weather forecast over complex orography: Sensitivity to the assimilation of conventional data. *Mon. Weather Rev.*, **131,** 136–154

Ferretti, R., Matrantonio, G., Argentini, S., Viola, A. and Santoleri, R. 2003a A model-aided investigation of a winter thermally driven circulation. *J. Geophys. Res.*, **108 D24,** 4777–4792

Ferretti, R., Paolucci, T., Giuliani, G., Cherubini, T., Bernardini, L. and Visconti, G. 2003b Verification of high-resolution real-time forecasts over the Alpine region during the MAP SOP. *Q. J. R. Meteorol. Soc.*, **129,** 587–607

Grell, G. A., Dudhia, J. and Stauffer, D. R. 1994 A description of the Fifth-Generation Penn State/NCAR Mesoscale Model (MM5). NCAR Technical Note NCAR/Tn-398+STR. National Center for Atmospheric Research, PO Box 3000, Boulder CO80307-3000, USA

Hong, Y. H. and Pan, H. L. 1996 Non-local boundary layer vertical diffusion in a medium range forecast model. *Mon. Weather Rev.*, **124,** 2322–2339

Kain, J. S. and Fritsch, J. M. 1990 A one-dimensional entraining/detraining plume model and its application in convective parameterization. *J. Atmos. Sci.*, **47,** 2784–2802

Liu, Z.-Q. and Rabier, F. 2003 The potential of high-density observations for numerical weather prediction: A study with simulated observations. *Q. J. R. Meteorol. Soc.*, **129,** 3013–3035

Massacand, A. C., Wernli, H. and Davies, H. C. 1998 Heavy precipitation on the Alpine south-side: An upper-level precursor. *J. Geophys. Res.*, **25,** 1435–1438

Medina, S. and Houze, R. A. 2003 Air-motion and precipitation growth in alpine storm. *Q. J. R. Meteorol. Soc.*, **129,** 345–372

Nuss, W. A. and Titley, D. W. 1994 Use of multiquadric interpolation for meteorological objective analysis. *Mon. Weather Rev.*, **122,** 1611–1631

Reisner, J., Rasmussen, R. J. and Bruintjes, R. T. 1998 Explicit forecasting of supercooled liquid water in winter storms using the MM5 mesoscale model. *Q. J. R. Meteorol. Soc.*, **124,** 1071–1107

Rotunno, R. and Ferretti, R. 2001 Mechanisms of intense alpine rainfall. *J. Atmos. Sci.*, **58,** 1732–1749

2003 Comparative analysis of rainfall in MAP cases IOP2b and IOP8. *Q. J. R. Meteorol. Soc.*, **129,** 373–390

Troen, I. and Mahrt, L. 1986 A simple model of the atmospheric boundary layer: Sensitivity to surface evaporation. *Boundary-Layer Meteorol.*, **37,** 129–148